

Tradeoff-mediated Drought Legacy in Soil Microbiome

Abstract

The irreplaceable, profound role of soil microbiome in driving biogeochemical cycling in the Earth System makes understanding its response to drought of increasing frequency and severity pivotal toward evaluating drought-mediated biosphere-atmosphere interactions. Drought legacy, a phenomenon of persistence of past effects that has been widely discussed in soil microbiome (and broadly in ecosystems), bears potentially far-reaching implications for carbon and nutrients cycling in ecosystems but with not yet fully resolved mechanism. Using a trait-based, mechanistically explicit microbial systems modelling framework, this study revealed an overarching tradeoff-mediated mechanism underpinning drought legacy in soil microbial systems decomposing organic matter. Rendered by the tradeoff between community drought tolerance and enzyme investment, drought legacy in microbial communities, either transient or persistent, is dependent on factors including among others drought intensity and microbial dispersal that can shape the tradeoff strength. These mechanistic insights into historical contingency of soil microbial community assembly and microbiome functioning hold tremendous promise to building a more prognostic science of microbiome. This study inspires us to coupling microbiome with vegetation with a holistic ecosystem view by capturing major tradeoff dimensions to evaluate and predict drought legacy in the biosphere.

1 Introduction

Drought of increasing severity and frequency both regionally and worldwide (**Borsa et al. 2014; Park Williams et al. 2020**) is one of the most pressing problems to the biosphere in general and to, specifically, microbiome in terrestrial ecosystems (**Berdugo et al. 2020**). The unparalleled role of soil microbiome in driving materials' cycling in the Earth system (**Falkowski et al. 2018**) makes understanding its response to drought crucial for completely evaluating drought impacts on the biosphere, which, however, is still largely missing or implicitly treated in global assessments of drought-biosphere interactions (e.g., **Green et al. 2019**). Over a-half century of research has uncovered physio-chemical, physiological, and ecological mechanisms explaining immediate impacts of drought on microbial systems functioning in soil environment (e.g., **Birch 1958, Schimel 2007; Manzoni et al. 2012**). However, it has been widely observed that drought effects with regards to microbiome functioning in terms of organic matter decomposition can persist when drought regimes change (e.g., **Evans and Wallenstein 2012; Meisner et al. 2015; Hawkes et al. 2017; Hinojosa et al. 2019**), a phenomenon termed drought legacy that has also been extensively discussed across the forest biome (e.g., **Anderegg et al. 2015; Johnstone et al. 2016; Conradi et al. 2020**). An intuitive question thus arises: what are the mechanisms underpinning drought legacy in organic matter decomposition? Elucidating the processes leading to drought legacy is undoubtedly essential for completely understanding microbial systems resilience and thus for quantifying carbon and nutrients cycling they significantly contribute to in the Earth System.

We propose an overarching trait-based, tradeoff-mediated mechanism from first principles to explain drought legacy in soil microbiome. Unambiguously, a drought legacy of changing organic matter decomposition is fundamentally rendered by persistence of the functional change of a microbial community. Such a functional change (induced by changes in extracellular enzymes)

is supposed to be achieved by a microbial community against the need to increase its community-level drought tolerance, which prompts a community-level tradeoff between drought tolerance and enzyme investment. These community-level changes emerge from physiological adaptation and turnover of individuals comprising the community in response to drought pressure. Physiologically, it is well established that a microbial cell directs resources to produce, for instance, osmolytes to combat desiccation (e.g., **Schimel 2007**), an intra-cellular metabolic plasticity that displays large inter-cellular variability (e.g., **Manzoni et al. 2012**). Quantifying these individual-level variations in traits (e.g., **Malik et al. 2019**), a trait-based, tradeoff-mediated mechanistic explanation emerges. With this top-down reasoning any factor that can eventually modify such a tradeoff from the bottom up may alter the property, magnitude, and duration of drought legacies. For instance, the intensity of drought, which directly modulates intracellular metabolic allocation (**Csonka 1989**), may shape the tradeoff. In addition, dispersal of microbes, a pivotal process in microbial community assembly by introducing taxa with new traits (**Vila et al. 2019**), is another factor that may alter drought legacy. Therefore, this trait-based, tradeoff-centric mechanistic framework is argued to explain the drought legacy phenomenon.

Past studies on soil microbiome drought legacy in soil carbon turnover have not yet tested trait-based rationale behind this phenomenon. Most of the studies, though having proposed some mechanisms, remained at the stage of loosely depicting compositional differences. Notably, **Hawkes and Keitt (2015)** proposed a mechanism of community-level shift in relative abundance of moisture generalist vs. specialist, of which generalist is functionally more stable than specialists with moisture. This idea was argued to explain the observation of a lack of change in moisture response across sites in Texas, USA because of observed dominance by generalist taxa resulting from high variation in rainfall (**Hawkes et al. 2017; Waring and Hawkes 2018**). Similarly, **Evans**

and Wallenstein (2014) argued from the point of view of life strategy to explain soils with relatively stable moisture history had more moisture-sensitive taxa and hence larger changes in biomass and composition (**Evans and Wallenstein** 2012). These proposed explanations, though intuitively appealing, still cannot really tell how a community is really shaped by historical drought disturbance and how its functional change can persist to enable drought legacy. This deficiency becomes especially apparent when having many studies reporting legacy of varying magnitudes with differing time scales, especially those that even did not observe a drought legacy at all (e.g., **Rousk et al. 2013; Fuchslueger et al. 2016**). Moreover, the potentially important role of microbial dispersal in influencing drought legacy was only briefly touched by **Hawkes et al. (2017)**, which again has not offer a more fundamental trait-based explanation. Therefore, past lab- and field-based efforts, though inspiring, are still far from being conclusive not only with regard to mechanistic details but also conceptually. To uncover more fundamental mechanisms underpinning and factors influencing drought legacy in microbiome, it is methodologically intrinsic to employ a bottom-up approach that can integrate individual-level mechanistic details and community-level interactions into microbial systems functioning.

Theory-driven trait-based modelling is well positioned to transcend limitations embedded in the current generation of lab- and field-based investigations. Individual-based microbial system modelling applying a trait-based approach is able to bridge across scales from individual cell through community to the system level to explicitly simulate ecological dynamics of microbial communities and emergent functioning (**Allison 2012**). Such a modelling approach is superior to the prevailing aggregated modelling approach of treating microbes as a single biomass pool [a review by **Wieder et al. (2015)**] in testing and uncovering the trait-based mechanisms. It offers a flexible modelling framework allowing building trait-based intra-cellular metabolic processes into

it and incorporating the tremendous taxonomic diversity, as well as examining microbial dispersal. Moreover, conducting modelling of legacy, trait-based investigations in particular, which has not yet been performed but instead suggested trivial in simulating functioning (e.g., **Rousk et al. 2013**), holds tremendous promise to moving forward microbial ecology toward a more predictive and prognostic direction by leveraging rich metagenomic data that could inform microbial traits (**Hatzenpichler et al. 2020**).

Is the trait-based, tradeoff-mediated mechanism underpinning soil microbiome drought legacy? This study addressed this overarching question using a mechanistically and spatially explicit trait- and individual-based soil microbial systems modelling framework—DEMENTpy. Specifically, these following questions were answered: can drought disturbance of varying severity all produce legacy effects in microbial systems manifested in organic matter decomposition? How would dispersal of microbes affect the formation of drought legacy? And what are the underlying changes in traits of drought tolerance and enzyme investment? We tackled these questions by applying the DEMENTpy to a grassland ecosystem in Southern California. This study would open up rich possibilities for more quantitative investigations into trait-based rules of soil microbial community assembly and into implications of legacies in microbial systems interacting with vegetation activities for the biosphere-atmosphere interactions.

2 Methods

2.1 Model description

DEMENTpy (DEcomposition Model of ENzymatic Traits in Python; GitHub Repository: <https://github.com/bioatmosphere/DEMENTpy>) is a spatially and mechanistically explicit trait- and individual-based microbial systems modelling framework built upon its predecessor

DEMENT (Allison 2012; Allison 2014; Allison and Goulden 2017; Wang and Allison 2019). This model randomly initializes a microbial community on a spatial grid based on various traits and simulates its dynamics by modelling explicitly demographic processes of each individual (including cell metabolism and growth, mortality, and reproduction) and their interactions under the influence of environmental factors of temperature and moisture at a daily time step, from which system-level functioning of decomposing substrates emerges (see **Supporting Fig. 1** for model structure). See the **Supporting Information** for more details with respect to overall structure, parameters, and functions.

With a trait-based approach, DEMENTpy creates a microbial community comprised of a large number of hypothetical taxa by randomly drawing values from uniform distributions of various microbial traits and assigning them to different taxa (see a list of traits in **Supporting Table 1** and more details in **Supporting Text**). Among the traits closely metabolism-associated are rates of enzyme production (constitutive and inducible) and rates of osmolyte production (constitutive and inducible). Drought tolerance of each taxon is determined by normalizing the inducible osmolyte rate of production to a value from 0 to 1. This treatment in a bottom-up fashion of starting from metabolic production of osmolyte and then determining drought tolerance is more biologically realistic (Schimel 2007), and updates the approach from the previous model version which instead directly introduced a drought tolerance parameter and imposed a penalty on carbon use efficiency accordingly (Allison and Goulden 2017).

Intra-cellular metabolic processing of carbon taken up from monomers generated from explicit degradation of substrates by extracellular enzymes are highlighted (see the **Supporting Text** for substrate degradation and other demographic processes). The metabolic processing of carbon assimilated after growth respiration is directed to produce enzyme (and respiration) and

osmolyte (and respiration; **Csonka 1989; Witteveen and Visser 1995**), which are treated as simultaneous processes without prescribing an order (**Supporting Fig. 3**). The carbon left after these processes accumulates toward biomass. We assume the constitutive osmolyte production rate varies across taxa without depending on water potential, accounting for bacterial/fungal cell's allocation of biomass to keep a water potential balance across cell wall (**Csonka 1989**). By contrast, inducible production of osmolytes is subject to constraints from water potential only when water potential reaches below a threshold. Arising from metabolic production of enzyme and osmolyte, mortality of microbial cells is simulated both deterministically by accounting for mass balance and stochastically based on death probability constrained by drought tolerance and water potential.

2.2 Modelling experiments

We deployed DEMENTpy (v1.0) to the grassland system at Loma Ridge, Southern California (**Allison et al. 2013**) and parameterized the model with 100 different hypothetical bacterial taxa on a 100 by 100 spatial grid decomposing grass litter containing ten different substrates (see parameter values in **Supporting Table 1** and substrates in **Supporting Table 2**). DEMENTpy is benchmarked with the daily weather data of year 2011, which is treated as the ambient scenario (**Supporting Fig. 4A**).

On top of this ambient scenario we conducted reciprocal simulations with manipulated drought to examine drought legacies (**Supporting Fig. 4**). Two drought scenarios, moderate and severe, were simply created by manipulating the magnitude of water potential across only the dry season linearly to four and ten times of ambient, respectively. Specifically, after drought disturbances of these two different scenarios the ambient scenario was successively imposed back to examine changes in microbial communities degrading substrates. One set of such simulations without dispersal is referred to as default mode. To further examine how dispersal affects drought

legacy, another dispersal model is set that can constantly introducing microbes from the microbial pool initialized at the onset of the simulations.

2.3 Simulation protocol and data analysis

With the model setup as above, we conducted simulations following the protocol as follows (**Supporting Fig. 4**): each simulation was run for 10 years at a daily time step after establishing an initial microbial community on the spatial grid, and in each new year substrates, monomers, and enzymes were reinitialized to have the same configurations as the very first year except for the microbial community. For the default mode, microbial community on the spatial grid in each new year is randomly moved around with an initialization strategy based on frequency of each taxon on the grid in the last day of the previous year (**Supporting Fig. 4C**). In contrast, in the dispersal mode the frequency was based on cumulative biomass of each taxon across the previous whole year (**Supporting Fig. 4D**). These simulations were repeated for each scenario under the two modes (default and dispersal mode) for 40 times with 40 different seeds. This sample size was determined by a convergence analysis of DEMENTpy's stochastic nature (**Supporting Fig. 5**). All results presented in this work, unless notified otherwise, were analyses of such an ensemble of 40 runs for each of the five scenarios ($5 \times 40 = 200$ runs in total).

From the outputs generated from these simulations data including microbes and substrates, as well as community-level traits (enzyme investment and drought tolerance) and community-level carbon allocation were extracted and calculated. See the **Supporting Text** for how calculations were done of community-level carbon allocation and traits of enzyme investment and drought tolerance. In addition, 95% confidence intervals were presented in most of the cases except for microbial community composition and community carbon allocation, for which results of only one out of the 40 simulations were shown.

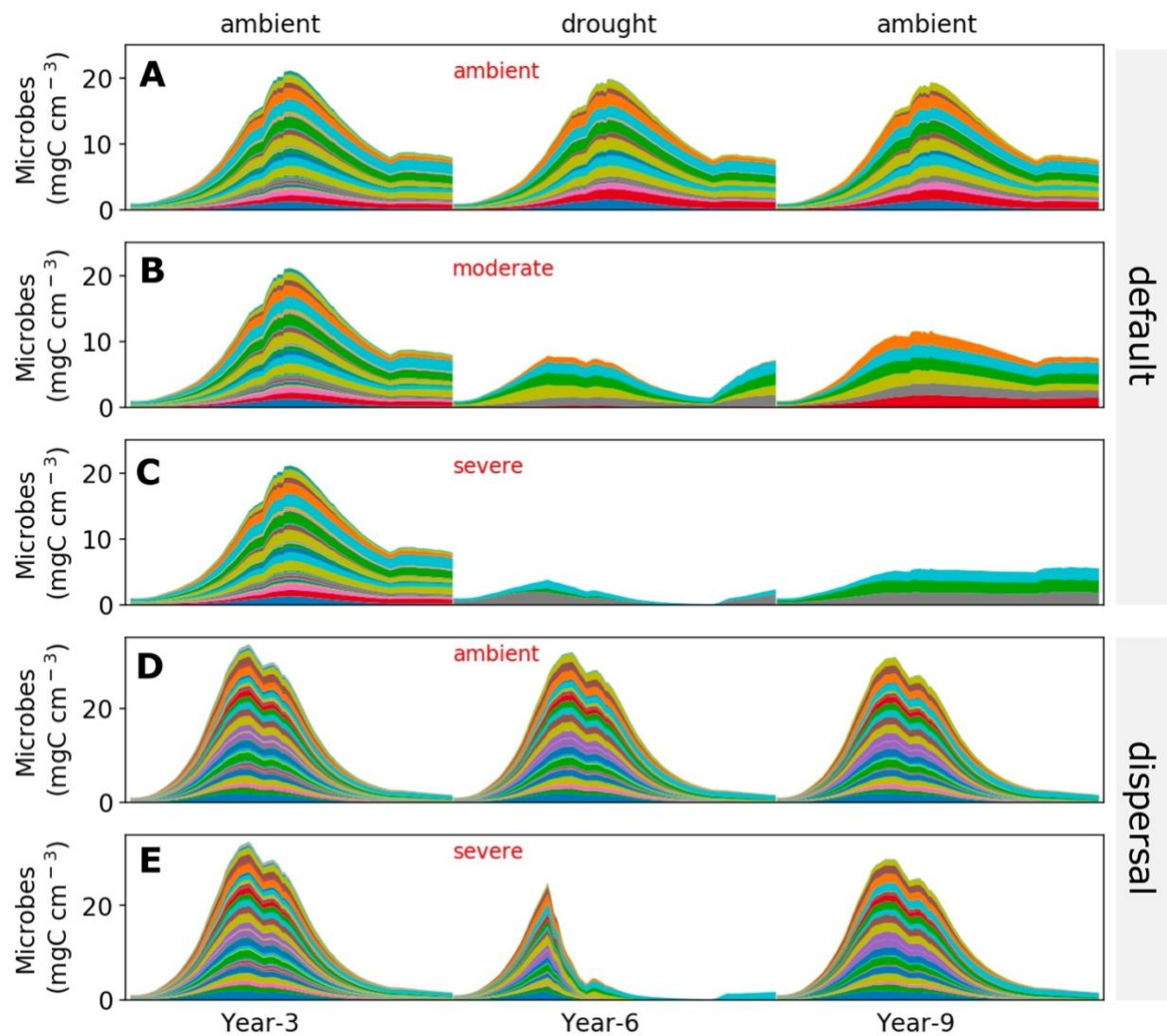


Fig.1. Microbial community dynamics disturbed by drought of differing severities with and without dispersal. (A-C) Dynamics without dispersal under ambient, moderate, and severe scenario, respectively. (D, E) Dynamics with dispersal under ambient and severe scenario, respectively. Colored bands represent different hypothetical taxa in terms of biomass (mg C cm⁻³) averaged over the 100×100 spatial grid. Data shown are only years 3, 6 (the 3rd year under drought), and 9 (the 3rd year after drought).

3 Results

3.1 Microbial community dynamics under the ambient drought scenario

The system became relatively stable after 2 years, with seasonal dynamics in the microbial community repeating across years (**Supporting Fig. 4**). Seasonal dynamics with respect to community composition and biomass reflected a joint control of environment and substrates. Starting from the wet season that was replete with substrates, a microbial community consisting of different taxa established and grew in biomass. As substrates were degraded and depleted, microbial cells began to starve and die. This was accompanied by increasing drought while entering the dry season, which induced more death. These two processes in combination resulted in the decline of microbial biomass after a biomass peak around 20 mg C cm⁻³ (**Fig. 1A**) and drove the compositional shift toward more taxa of higher drought tolerance and less lower enzyme investment (**Supporting Fig. 5A**). Similar seasonal and inter-annual dynamics were observed for the community with dispersal but with much higher biomass (peaked around 30 mg C cm⁻³) and taxonomic diversity (**Fig. 1D; Supporting Fig. 5B**).

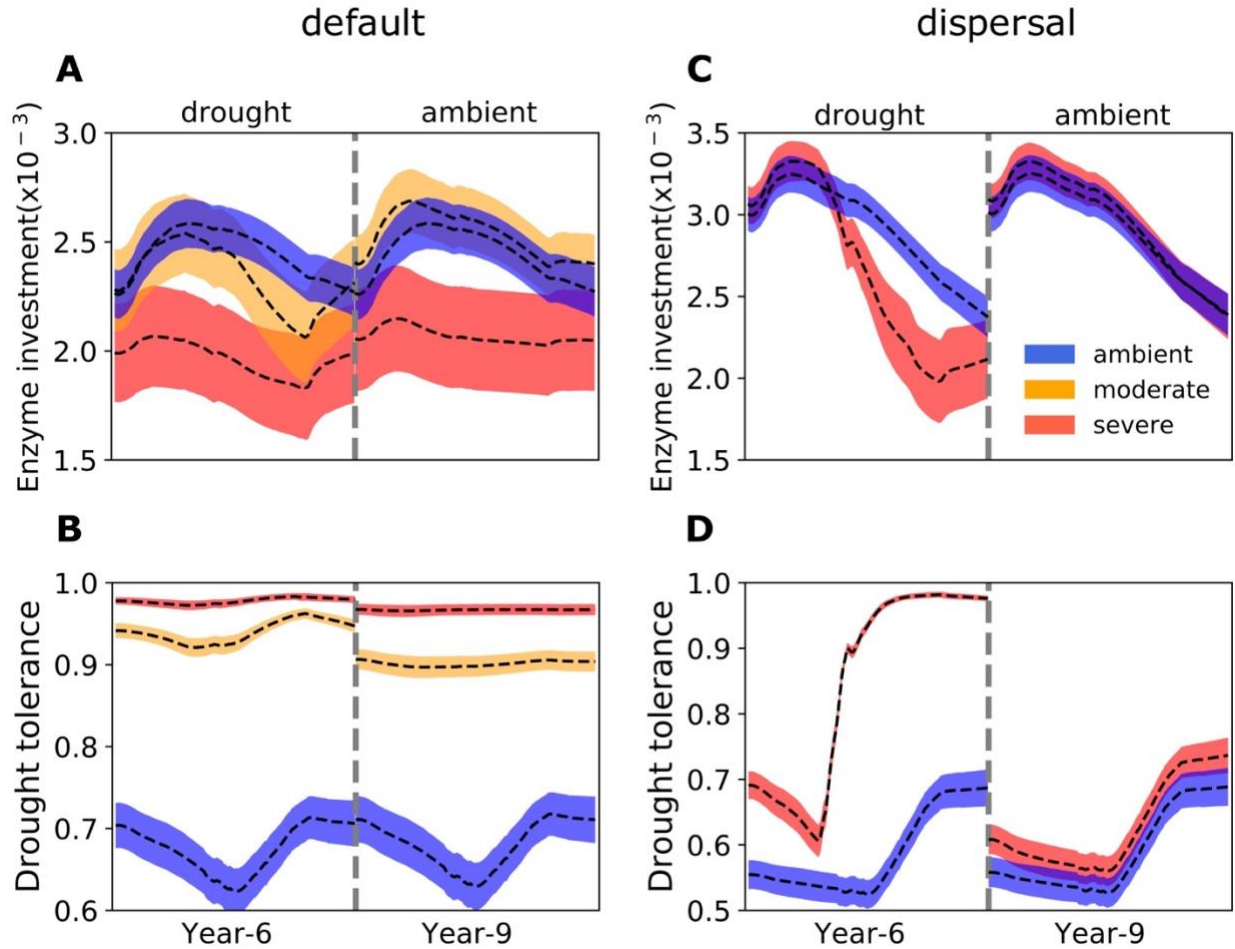


Fig.2 Seasonal dynamics of community-level traits of enzyme investment and drought tolerance of stabilized communities under different drought scenarios. (A, B) Enzyme investment and drought tolerance of year 6 (3rd year under drought) and year 9 (3rd year after drought) under three scenarios (ambient, moderate, and severe) without dispersal, respectively. **(C, D)** The same for communities with dispersal under two scenarios (ambient and severe). Dashed lines and color bands are means and confidence intervals (95%) based on 40 runs of each of the 5 scenarios.

3.2 Responses to and recoveries from drought disturbance of varying severity

The exerted drought of two differing severities altered the microbial community to varying extents (**Fig. 1B, C**). Total biomass declined significantly, with the severe scenario displaying the most by about 50% to a peak less than 10 mg C cm⁻³. Composition of the communities changed dramatically in terms of taxonomic richness and abundance, forming new alternative stable communities after 2 years of drought perturbation that hold differing community-level drought tolerance and enzyme investment. Compared to the ambient scenario, although the drought tolerance increased significantly across the whole season from as low as only 0.62 to 0.92 of the moderate scenario and to 0.97 of the severe, the community enzyme investment only declined significantly in the severe scenario across the dry season and in the moderate scenario did not change much on average besides the later stage in dry season (**Fig. 2A,B**). These community-level traits' changes dictated differences in community level carbon allocation between enzymes and osmolytes and thus yield (**Fig.3A**). Under the moderate scenario, the percentage of carbon assimilated allocated to osmolytes ranged between 65–85%, compared to the ambient range of 50–70% in, whereas the enzymes' allocation was consistently lower (10% on average) than the ambient (20% on average). However, the resulting yield was basically similar, ranging between 0 - 30%, though a few points in the ambient were higher (reaching at most 40%) early in the drought season. Under the severe scenario, the percentage of osmolytes became even higher and enzymes even lower, and the community yield approached zero more often. Eventually, these differences in community resource allocation between osmolytes and enzymes were manifested in the dampened degradation of substrates over the grid, with the two drought scenarios resulting in different levels of decomposition declines (an average by 57.39 and 85.65%, respectively; **Fig.4A, B**).

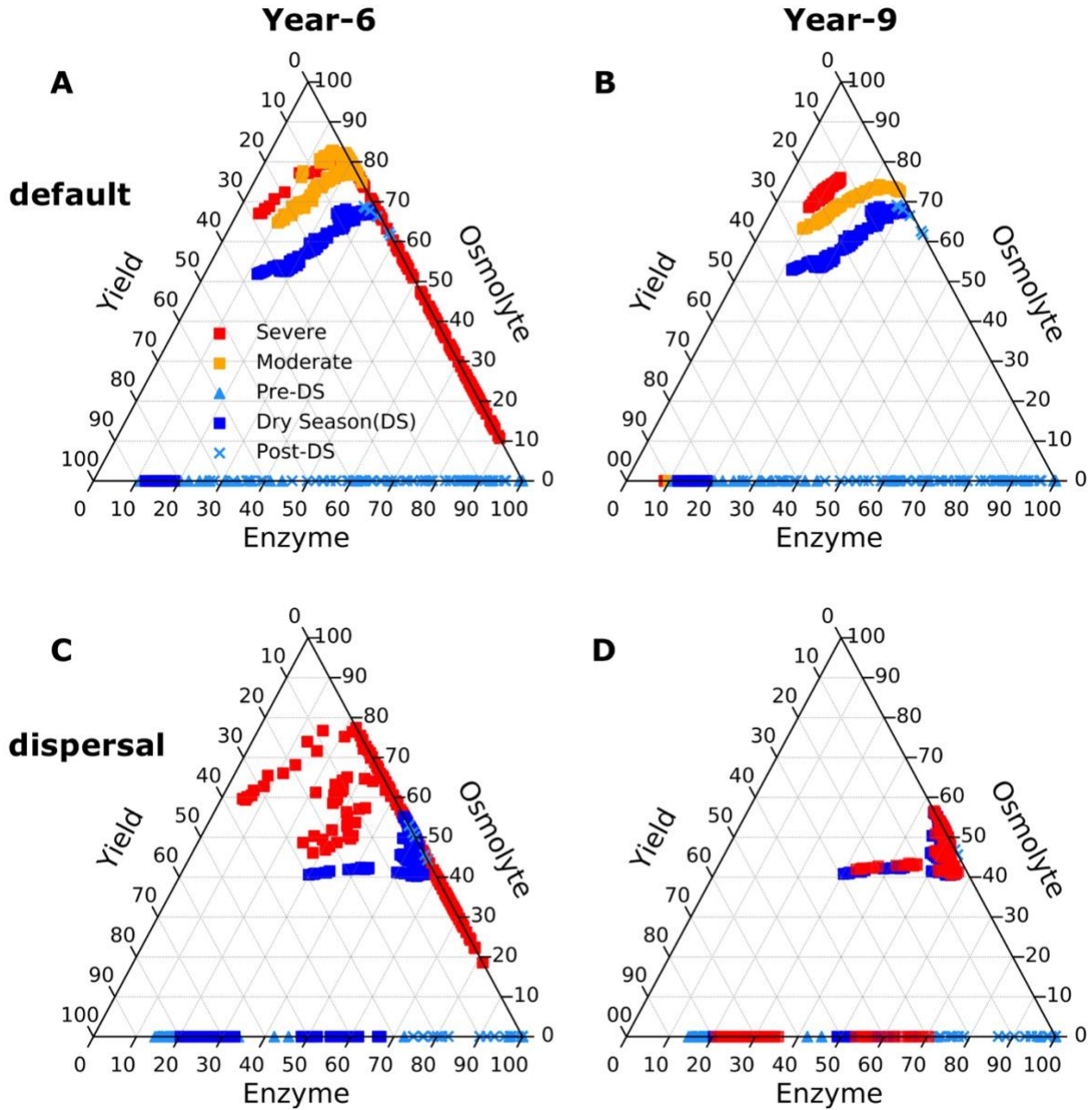
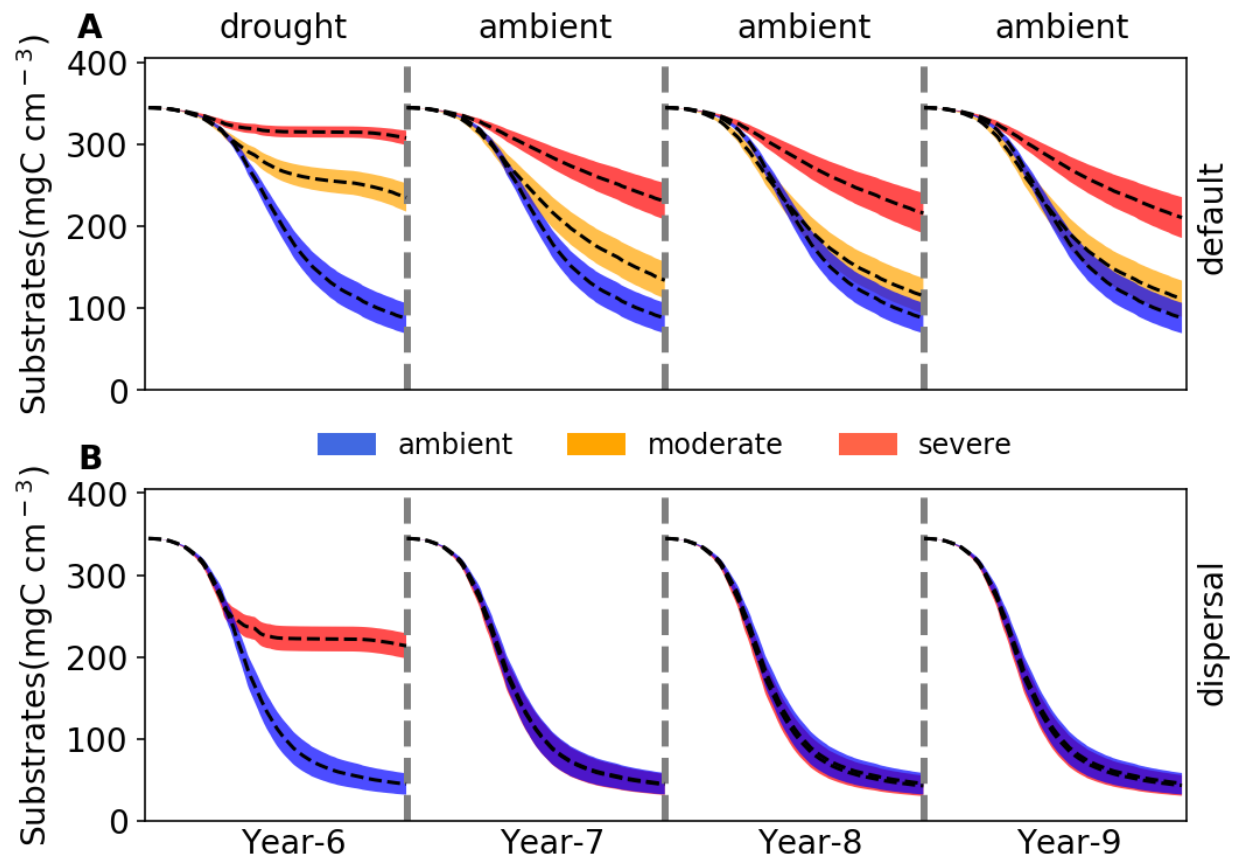


Fig.3 Ternary plots of community-level allocation of assimilated carbon among enzymes, osmolytes, and yield over season under different drought scenarios. (A, B) Enzyme-Osmolyte-Yield tradeoff of communities over year 6 (3rd year under drought) and year 9 (3rd year after drought), respectively, of the default mode (without dispersal). (C, D) The same for the dispersal mode. Besides the ambient cases (both default and dispersal mode) illustrating the whole season, moderate and severe scenarios were only shown with the data of dry season. [NOTE: the

discontinuities under ambient arose from prescribing a water potential threshold, above which osmolytes are produced at a constant constitutive rate and a constant basal inducible rate (that's why we see pre- and post-dry season mostly had fairly low but NOT zero osmolytes), and below which inducible osmolytes' production is dependent on water potential. These have been detailed in the methods and more will be listed in the supplementary]

When the ambient scenario was imposed back, after 2 years (year 9) new stable microbial communities formed and persisted (**Fig. 1B, C** and **Supporting Fig. 4C**). Compared to the ambient scenario, these newly formed alternative stable communities had differing drought tolerance and enzyme investment (**Fig. 2A, B**). Drought tolerance was significantly higher under both the moderate (0.90) and severe scenario (0.96) than under the ambient, though both became a little lower than the communities realized under drought disturbance. In contrast, enzyme investment under the moderate scenario became similar to the ambient community, with only the severe scenario community remaining significantly different. These changes were reflected in the results of only the severe community showing a clearly lower allocation to enzymes than the ambient community across the dry season (**Fig. 3B**). This loss of differences in enzyme investment in the moderate community eventually resulted in only the severe scenario displaying significantly reduced degradation compared to the ambient scenario (an average by 47.72%; **Fig. 4B**), although the magnitude of decline was dampened compared to the antecedent drought period because of the relief of drought pressure (**Fig. 4A**). It is noteworthy that prior to the alternative stable states, the degradation changes resulting from the transient communities (year 7) were significant for both of drought scenarios (an average decline by 18.00 and 55.52%, respectively).

272



273

274

275

276

277

278

279

280

281

282

283

Fig. 4 Changes in substrates driven by drought. (A) Total substrates on the spatial grid over year 6-9 under three different scenarios (ambient, moderate, and severe) without dispersal. (B) The same for simulations with dispersal under only ambient and severe scenarios. Dashed lines and colored bands are means and confidence intervals (95%), respectively, based on 40 runs for each of the five scenarios.

3.3 Responses to and recoveries from the severe drought disturbance with dispersal

With dispersal the stable microbial community realized under the severe scenario saw both declined total biomass and declined taxonomic abundance, particularly significant during the dry season (**Fig. 1E**). This stable community held significantly different community enzyme

investment and drought tolerance from the ambient. Enzyme investment and drought tolerance declined (from 0.0033 to 0.0020) and increased (from 0.60 to 0.97) sharply across the dry season, respectively, enlarging their differences from the ambient over time (**Fig. 2C,D**). These changes resulted in the community allocating more assimilated carbon to produce osmolytes and less to enzymes, which even resulted in zero yield when drought was too severe across the dry season (**Fig. 3C**). All these changes pointed to significant declines in decomposition of substrates (an average decline by 56.29%; **Fig. 4C**)

However, when the ambient drought was imposed back, recovery from the drought was dramatically complete. After 2 years the stabilized community became the same as the ambient (**Fig. 1E**). This compositional indifference was illustrated axiomatically by the same community enzyme investment (**Fig. 2C**) and drought tolerance (**Fig. 2D**), the same community-level allocation of assimilated carbon among enzymes (30 - 60%), osmolytes (40 - 60%), and thus yield (0 - 30%; **Fig. 3D**), and eventually the almost completely same substrates' decomposition (**Fig. 4D**). In contrast to the default mode, the transient community did not show significant effects in the 1st year after drought (year 7; **Fig. 4D**).

4 Discussion

With a trait-based modelling approach in a mechanistically explicit fashion, this study examined relationships between drought legacy and factors of drought severity and dispersal in microbiome in the terrestrial ecosystem setting. Drought legacy can manifest at the system level in terms of litter decomposition, as clearly illustrated by the impaired decomposition after experiencing drought disturbance (**Fig. 4B**). However, drought legacy is contingent on drought

severity and microbial dispersal, pointing to a more overarching mechanistic notion underpinning drought legacy in soil microbiome.

4.1 Intensity-contingent alternative stable systems and drought legacies

Based on an assumption of a realization of stable state under drought disturbance, the severity of drought disturbance matters in the magnitude and duration of legacy formed. We argue this assumption is a reasonably good starting point, which in reality is not always the case for sure considering huge variations in terms of frequency, intensity, and duration of drought. Intensity of past drought determines the extent to which a microbial community can adapt to the drought, thereby shaping varying transient and new alternative stable states (**Fig. 1B,C**). A change in decomposition is fundamentally dictated by functional differences in the underlying communities. These legacy-induced new alternative stable states hold differing capability of organic matter decomposition, especially in the new alternative stable states, arising from different drought disturbances. Drought disturbance of a relatively low severity, though being able to result in a declined decomposition immediately conferred by the transient community (which we dub transient legacy), induced a new stable community that is compositionally different but functionally similar in decomposing litters (**Fig. 4A**). This transient legacy matches the field experiment at the same site very well that observed mitigated drought legacy in terms of litter decomposition within three years (**Martiny et al. 2017**). The compositional but not functional change in the new stable alternative system reflects a broad notion of functional redundancy in soil microbiome (**Allison and Martiny 2008**), which was widely observed in other natural systems (e.g., **Fukami 2015**). Meanwhile, this decomposition indifference excluded the role of biomass difference (a peak biomass decline by as high as 50% under the moderate scenario; **Fig. 1B**), which is in consistent with findings from a reciprocal transplant study across a climate gradient by

Glassman et al. (2019). Rather, drought in a less intense degree, though being able to increase community drought tolerance, is not strong enough to change enzyme investment in the new stable community (**Fig. 2A, B**). In contrast, stronger drought can push the community to reach an even higher drought tolerance by sacrificing more of capability in enzyme investment, which resulted in a persistent drought legacy in organic matter decomposition (**Fig. 4B**). Similar historical contingency of alternative stable system with a functional difference was also observed in gut microbiota experiencing transient osmotic perturbation (**Tropini et al. 2018**) and in forest biome globally (tropical forest: **Hirota et al. 2011**; **Staver et al. 2011**; boreal forest: **Herzschuh 2019**).

4.2 Indispensable role of dispersal in drought legacy

New alternative stable systems shaped by drought of differing severity, though being able to last and carry the legacy effects into the future, are faced with other disturbances and thereby subject to changes. Dispersal is one such process that can negate formation of alternative stable systems and drought legacies. By constantly introducing taxa from the same microbial pool, results with even the most severe drought scenario demonstrated that dispersal can completely dampen the drought-driven selection on a microbial community, thus overwhelming the drought legacy because of community-level similarities in drought tolerance and enzyme investment (**Fig. 4B**). It is noteworthy that dispersal is a complicated process. Factors in dispersal influencing resident community are manifold (**Vila et al. 2019**); for instance, timing (**Fukam 2015**) and velocity (**Evans et al. 2019**) both have been suggested to be important. Moreover, even an unsuccessful dispersal with only transient interactions can induce an alternative stable state functioning differently (**Amor et al. 2020**). The scenario examined in this study by no means is exclusive, but it represents a plausible condition for the purpose of uncovering underlying mechanisms. Responding to those variations in the dispersal process, microbial systems could present different

stable systems and varying magnitudes of changes in decomposition, which warrant more explorations.

4.3 Tradeoff (strength) governing drought legacy

From the contrasts of cases of low vs. high drought severity and of cases with vs. without dispersal, we can arguably deduce that drought legacy in microbiome functioning is fundamentally determined by the strength of tradeoff between drought tolerance and enzyme investment. For instance, when drought stress is low (**Fig. 4A**) or dispersal overwhelms drought-driven community adaptation (**Fig. 4B**), the community-level tradeoff is not strong enough to enable drought legacy to eventually occur, even if with transient legacy. In contrast, when enough tradeoff strength is reached, a community shift towards an increasing abundance of drought-tolerant taxa to reach increasing drought tolerance by sacrificing capacity of enzyme production will result in impaired capability in degrading substrates.

However, mechanisms and factors influencing strength of the tradeoff between the community-level enzyme investment and drought tolerance are complex and manifold. In fact, tradeoffs in microbiome and beyond are complex in general (e.g., **Berezovsky & Shakhnovich, 2005; Ferenci 2016**). Notably, tradeoffs are not necessarily rigid, which may even be the opposite of a tradeoff (e.g., **Tikhonov et al. 2020**). Such complexities can be rendered by factors including among others drought intensity, dispersal, and potentially many other unknown processes. Therefore, broadening the scope of scenarios examined in this study (as discussed earlier) and/or relaxing assumptions in DEMENTpy offers natural directions in which our study can be extended for exploring more tradeoff-mediated mechanisms underpinning drought legacy. Meanwhile, this tradeoff notion raises a broad question of how to quantify tradeoff strength constrained by traits' space in microbiome, which is expected to be a fruitful research avenue. Additionally, extending

this tradeoff-mediated drought legacy mechanism to larger spatial scales across different systems would be another fruitful direction. In summary, it's highly expected that insights gained from these tradeoff strength-oriented inquiries not only can reconcile the huge discrepancies across studies in different systems with respect to property, magnitude, and duration but also would uncover tempo-spatial patterns.

4.4 Implications for soil and ecosystem

Tradeoff-mediated drought legacies emerging from trait-based microbial community shifts bear immediate implications for understanding soil microbiome and broad consequences for quantifying ecosystems' responses and feedbacks to increasing frequency and severity of drought and other environmental changes. Depicting tradeoffs and quantifying their strength in studying whether and how history of drought can shape alternative stable systems in microbiome contributes to fundamental understanding of microbial community assembly from a tremendous taxonomic diversity and to quantifying the magnitude and duration of drought legacy. For instance, a legacy of impaired decomposition, either transient or persistent, may enhance carbon sequestration in soil systems at certain temporal scales, but may also allow fuels to accumulate for the next fire season, thereby increasing fire risk (e.g., **Pellegrini et al. 2017**). Additionally, impaired decomposition can inhibit release of nutrients from detritus and thus their return to plants, influencing plant-microbe interactions (e.g., **Legay et al. 2018**). All these and potentially many other cascading changes arising from microbiome legacy would engender more complex feedbacks in ecosystems. Evaluating their implications entails an integrative, holistic view of components in systems across ecosystem and the Earth System scales. To proceed, this study clearly indicates that to really establish a predictive science of carbon cycling in ecosystems in the context of projected global

climate change, considering history as an essential component means that dimensions and spaces of essential tradeoffs should be incorporated, and this trait-based modelling study offers an inspirational starting point for moving forward in this direction.

References

Allison, S. D. (2012). A trait-based approach for modelling microbial litter decomposition. *Ecology letters*, 15, 1058-1070.

Allison, S. D., Lu, Y., Weihe, C., Goulden, M. L., Martiny, A. C., Treseder, K. K., & Martiny, J. B. (2013). Microbial abundance and composition influence litter decomposition response to environmental change. *Ecology*, 94, 714-725.

Berezovsky, I. N., & Shakhnovich, E. I. (2005). Physics and evolution of thermophilic adaptation. *Proceedings of the National Academy of Sciences*, 102, 12742-12747.

Birch, H. F. 1958. The effect of soil drying on humus decomposition and nitrogen availability. *Plant and Soil*, 10, 9–31.

Borsa, A. A., Agnew, D. C., & Cayan, D. R. (2014). Ongoing drought-induced uplift in the western United States. *Science*, 345, 1587-1590.

419 Conradi, T., Van Meerbeek, K., Ordonez, A., & Svenning, J. C. (2020). Biogeographic historical
 420 legacies in the net primary productivity of Northern Hemisphere forests. *Ecology Letters*.
 421 <https://doi.org/10.1111/ele.13481>
 422
 423 Csonka, L. N. (1989). Physiological and genetic responses of bacteria to osmotic stress.
 424 *Microbiological Reviews*, 53, 121-147.
 425
 426 Cuddington, K. (2011). Legacy Effects: The Persistent Impact of Ecological Interactions.
 427 *Biological Theory*, 6, 203–210.
 428
 429 Evans, S.E., Wallenstein, M.D. (2012) Soil microbial community response to drying and rewetting
 430 stress: does historical precipitation regime matter? *Biogeochemistry*, 109, 101–116.
 431
 432 Falkowski, P. G., Fenchel, T., & Delong, E. F. (2008). The microbial engines that drive Earth's
 433 biogeochemical cycles. *Science*, 320, 1034-1039.
 434
 435 Ferenci, T. (2016). Trade-off mechanisms shaping the diversity of bacteria. *Trends in*
 436 *Microbiology*, 24, 209-223.
 437
 438 Gommers, P. J. F., Van Schie, B. J., Van Dijken, J. P., & Kuenen, J. G. (1988). Biochemical limits
 439 to microbial growth yields: an analysis of mixed substrate utilization. *Biotechnology and*
 440 *Bioengineering*, 32, 86-94.
 441

- Green, J.K., Seneviratne, S.I., Berg, A.M. *et al.* (2019). Large influence of soil moisture on long-term terrestrial carbon uptake. *Nature*, 565, 476–479.
- Herzschuh, U. (2020). Legacy of the Last Glacial on the present-day distribution of deciduous versus evergreen boreal forests. *Global Ecology and Biogeography*, 29, 198-206
- Hinojosa, M. B., Laudicina, V. A., Parra, A., Albert-Belda, E., & Moreno, J. M. (2019). Drought and its legacy modulate the post-fire recovery of soil functionality and microbial community structure in a Mediterranean shrubland. *Global Change Biology*, 25, 1409-1427.
- Hobbie, J. E., & Hobbie, E. A. (2013). Microbes in nature are limited by carbon and energy: the starving-survival lifestyle in soil and consequences for estimating microbial rates. *Frontiers in Microbiology*, 4, 324.
- Johnstone, J. F., Allen, C. D., Franklin, J. F., Frelich, L. E., Harvey, B. J., Higuera, P. E., ... & Schoennagel, T. (2016). Changing disturbance regimes, ecological memory, and forest resilience. *Frontiers in Ecology and the Environment*, 14, 369-378.
- López-Urrutia, Á., & Morán, X. A. G. (2007). Resource limitation of bacterial production distorts the temperature dependence of oceanic carbon cycling. *Ecology*, 88, 817-822.
- Manzoni, S., Schimel, J. P., & Porporato, A. (2012). Responses of soil microbial communities to water stress: results from a meta-analysis. *Ecology*, 93, 930-938.

465 Meisner, A., Rousk, J., & Bååth, E. (2015). Prolonged drought changes the bacterial growth
 466 response to rewetting. *Soil Biology and Biochemistry*, 88, 314-322.

467

468 Sardans, J., & Peñuelas, J. (2010). Soil enzyme activity in a Mediterranean forest after six years
 469 of drought. *Soil Science Society of America Journal*, 74, 838-851.

470

471 Schimel, J., Balser, T. C., & Wallenstein, M. (2007). Microbial stress-response physiology and its
 472 implications for ecosystem function. *Ecology*, 88, 1386-1394.

473

474 Schimel, J. P., & Weintraub, M. N. (2003). The implications of exoenzyme activity on microbial
 475 carbon and nitrogen limitation in soil: a theoretical model. *Soil Biology and Biochemistry*, 35,
 476 549-563.

477

478 Sinsabaugh, R. L., Manzoni, S., Moorhead, D. L., & Richter, A. (2013). Carbon use efficiency of
 479 microbial communities: stoichiometry, methodology and modelling. *Ecology Letters*, 16, 930-939.

480

481 Tiemann, L. K., & Billings, S. A. (2011). Changes in variability of soil moisture alter microbial
 482 community C and N resource use. *Soil Biology and Biochemistry*, 43, 1837-1847.

483

484 Wang, B., & Allison, S. D. (2019). Emergent properties of organic matter decomposition by soil
 485 enzymes. *Soil Biology and Biochemistry*, 136, 107522.

486

487 **Acknowledgements**

488 ...

489

490

491

492

493

494

495

496

497

498

499

500

501

502

503

504

505

506

507

508

Supporting Information

Tradeoff-mediated Drought Legacy in Soil Microbiome

Bin Wang, Steven D. Allison

1 DEMENTpy

DEMENTpy, an explicit microbial systems modelling framework both mechanistically and spatially, is an effort of mechanistically updating (see **Supporting Fig. 1** for conceptual structure) and programmatically restructuring DEMENT (see **Supporting Fig. 2** for programming structure. The source code is archived at <https://github.com/bioatmosphere/DEMENTpy>. Processes simulated in DEMENTpy are described briefly below.

1.1 Microbial community initialization

With a trait-based approach, a microbial pool comprised of a large number of hypothetical taxa in DEMENTpy is created by randomly drawing values from distributions of various microbial and enzymatic traits (**Supporting Table 1**) and assigning them to different taxa. These proxy taxa with differing combinations of traits' values are placed on the spatial grid to form a spatially-explicit microbial community [see Wang and Allison (2019) to get a better notation of its of spatial feature]. Trait distributions are all assumed to follow uniform distributions, except that for simplicity, some traits are assumed to be constants, and values of some traits are derived from established correlations with other traits. These distributions and assumptions are largely informed by field- and lab-based experimental works (**Allison 2012; Allison and Goulden 2017**).

Four of the major traits determining intra-cellular metabolism of enzyme and osmolyte and thus mass balance are rates of enzyme production (constitutive and inducible) and rates of osmolyte production (constitutive and inducible). The rate of production of inducible osmolyte is

then normalized to a value from 0 to 1, which is regarded as drought tolerance. Such a treatment of drought tolerance is in contrast to the drought tolerance trait adopted in a previous version which instead directly introduced a drought tolerance parameter and imposed a penalty on carbon use efficiency accordingly (**Allison and Goulden 2017**). This update in a bottom-up fashion of starting from osmolyte production and then determining drought tolerance is supposed to be more biologically realistic.

1.2 Metabolic production of enzyme and osmolyte

Different individuals comprising the microbial community finish their demographic processes of growth, mortality, and reproduction while degrading substrates and taking up monomers under the influence of temperature and water potential. From these underlying processes emerges dynamics and functioning at both the microbial cell level and the whole system level.

Degradation of substrates are calculated explicitly by using different enzymes with different kinetic properties. One principle during the simulation is that every substrate at least has one enzyme to degrade and vice versa. Different monomers are calculated explicitly by having differing transporters to target them. Transporters of different types and amounts are taxon-specific, which is described immediately below. The governing equation of both substrates' degradation and monomers' uptake follows the Michaelis-Menten equation, which is further constrained by temperature (accounting for temperature impacts on enzymatic kinetics) and water potential (accounting for enzymatic kinetics and diffusion declines arising from drought; **Allison and Goulden 2017**):

$$V = \frac{V_{max}f(T)[S][E]}{K_m + [S]} f(\psi)$$

$$f(T) = e^{\left(-\frac{\epsilon}{R}\left(\frac{1}{T} - \frac{1}{T_{ref}}\right)\right)}$$

$$f(\psi) = e^{k\psi}$$

where E and S represent enzyme and substrate concentration, respectively, V_{max} represents the enzyme catalytic constant, K_m denotes the concentration of S at which V is one half V_{max} , ϵ is enzymatic activation energy, R is universal gas constant, and k is a coefficient controlling sensitivity to water potential which distinguishes between degradation and uptake.

Intra-cellular production of enzyme and osmolytes are described below in detail with respect to simulation methods and their underlying rationales. Metabolism explicitly deals with both the carbon upon uptake from degraded substrates and the carbon in biomass of microbial cells inducibly and constitutively (**Supporting Fig. 3**). The metabolic processing of carbon assimilated after growth respiration is allocated to enzyme production (and respiration) and osmolyte production (and respiration; **Csonka 1989; Witteveen and Visser 1995**), which are treated horizontally in the model without prescribing an order. The C left after these processes accumulates toward biomass. We assume the constitutive osmolyte production rate ($Osmo_Con$) varies across taxa without depending on water potential, accounting for bacterial/fungal cell's allocation of biomass to keep a water potential balance across cell wall (**Csonka 1989**). By contrast, taxon-specific inducible production of osmolytes ($Osmo_Ind$) is subject to constraints from water potential and is calculated following:

$$Osmo_{Ind}(i) = \begin{cases} Osmo_Indi, & Psi \geq \psi_{th} \\ Osmo_Indi (1 - \alpha Psi), & Psi < \psi_{th} \end{cases}$$

where $Osmo_Indi$, indexed by taxon i, is the i th taxon's osmolyte production rate, Psi is the daily water potential, α is a rate constant, and ψ_{th} is a system water potential constant, below which inducible osmolyte production is activated. Though with a differing production rate across taxa,

osmolytes in the current version are assumed to hold a constant stoichiometry of C and N, which governs consumption of N in intracellular metabolism.

Arising from metabolic production of enzyme and osmolyte, mortality of microbial cells is simulated both deterministically by accounting for mass balance and stochastically based on death probability constrained by drought tolerance and water potential, of which taxon-specific mortality probability is calculated following:

$$Mort_i = Death_basal_i[1 - Death_rate_i(1 - Tol_i)(Psi - \psi_{th})]$$

where $Death_basal_i$ is Taxon $_i$'s basal mortality probability, $Death_rate_i$ is a coefficient, and Tol_i is drought tolerance. Microbial cells that are either out of mass balance or randomly killed are designated as dead ones, removed from the microbial community, and added into the substrates pools as dead microbes. Microbial reproduction is simply calculated by splitting microbes into two halves, which disperse to surrounding grid boxes on the spatial grid.

References

Allison, S. D. (2012). A trait-based approach for modelling microbial litter decomposition. Ecology letters, 15, 1058-1070.

Allison, S. D., & Goulden, M. L. (2017). Consequences of drought tolerance traits for microbial decomposition in the DEMENT model. Soil Biology and Biochemistry, 107, 104-113.

600 Wang, B., & Allison, S. D. (2019). Emergent properties of organic matter decomposition by soil
601 enzymes. *Soil Biology and Biochemistry*, 136, 107522.
602
603

Supporting Table 1 Major microbial and enzyme parameters and their values

Parameter	Value	Unit	Note
max_size_b	2	mg cm-3	C quota threshold for bacterial cell division
Cfrac_b	0.825	mg mg-1	Bacterial C fraction
Nfrac_b	0.16	mg mg-1	Bacterial N fraction
Pfrac_b	0.015	mg mg-1	Bacterial P fraction
Crange	0.09	mg mg-1	Tolerance on C fraction
Nrange	0.04	mg mg-1	Tolerance on N fraction
Prange	0.005	mg mg-1	Tolerance on P fraction
C_min	0.086	mg cm-3	threshold C concentration for cell death
N_min	0.012	mg cm-3	threshold P concentration for cell death
P_min	0.002	mg cm-3	threshold C concentration for cell death
Uptake_C_cost_min	0.01	transporter mg-1 biomass C	Minimum per enzyme C cost as a fraction of uptake
Uptake_C_cost_max	0.1	transporter mg-1 biomass C	Maximum per enzyme C cost as a fraction of uptake
Uptake_Maint_cost	0.01	mg C transporter-1 day-1	Respiration cost of uptake transporters
Enz_per_taxon_min	0		Minimum number of enzymes a taxon can produce
Enz_per_taxon_max	40		Maximum number of enzymes a taxon can produce
Enz_Prod_min	0.00001	mg C mg-1 day-1	Minimum per enzyme production cost as a fraction of C uptake rate
Enz_Prod_max	0.0001	mg C mg-1 day-1	Maximum per enzyme production cost as a fraction of C uptake rate
Constit_Prod_min	0.00001	mg C mg-1 day-1	Minimum per enzyme production cost as a fraction of biomass C
Constit_Prod_max	0.0001	mg C mg-1 day-1	Maximum per enzyme production cost as a fraction of biomass C
Osmo_per_taxon_min	1		Minimum number of osmolyte a taxon can produce
Osmo_per_taxon_max	1		Maximum number of osmolyte a taxon can produce
Osmo_Consti_Prod_min	0.0000001	mg C mg-1 day-1	Minimum per osmolyte production cost as a fraction of biomass C
Osmo_Consti_Prod_max	0.000001	mg C mg-1 day-1	Maximum per osmolyte production cost as a fraction of biomass C
Osmo_Induci_Prod_min	0.01	mg C mg-1 day-1	Minimum per osmolyte production cost as a fraction of C uptake rate
Osmo_Induci_Prod_max	0.1	mg C mg-1 day-1	Maximum per osmolyte production cost as a fraction of C uptake rate
CUE_ref	0.5	mg mg-1	Growth efficiency at the reference temperature
CUE_temp	-0.005	mg mg-1	Growth efficiency change with enzyme investment
death_rate_bac	0.001		Bacterial death rate
basal_bac	10		Bacterial basal death probability
wp_th	-2		water potential threshold at which osmolyte is induced
alpha	0.01		Osmolyte production change with water potential
Vmax0_min	5	mg substrate mg-1 enzyme day-1	Minimum Vmax for enzyme
Vmax0_max	50	mg substrate mg-1 enzyme day-1	Maximum Vmax for enzyme

Uptake_Vmax0_min	1	mg substrate mg-1 substrate day-1	Minimum uptake Vmax
Uptake_Vmax0_max	10	mg substrate mg-1 substrate day-1	Maximum uptake Vmax
Uptake_Ea_min	35	kJ mol-1	Minimum activation energy for uptake
Uptake_Ea_max	35	kJ mol-1	Maximum activation energy for uptake
Km_min	0.01	mg cm-3	Minimum Km
Uptake_Km_min	0.001	mg cm-3	Minimum uptake Km
Vmax_Km	1	mg enzyme day cm-3	Slope for Km-Vmax relationship
Vmax_Km_int	0	mg cm-3	Intercept for Km-Vmax relationship
Uptake_Vmax_Km	0.2	mg biomass day cm-3	Slope for uptake Km-Vmax relationship
Uptake_Vmax_Km_int	0	mg cm-3	Intercept for uptake Km-Vmax relationship
Specif_factor	1		Efficiency-specificity

616

Supporting Table 2 Substrate concentrations initialized in
DEMENT simulations (mg cm⁻³).

Substrate	C	N	P
DeadMic	0	0	0
DeadEnz	0	0	0
Cellulose	146.89	0	0
Hemicellulose	85.855	0	0
Starch	12.21	0	0
Chitin	4.9952	0.83254	0
Lignin	48.51	0.40425	0
Protein1	10.6	2.09704	0
Protein2	10.6	2.09704	0
Protein3	10.6	2.09704	0
OrgP1	12.48	0	0.478469
OrgP2	1.8182	0.79745	0.478469

617

618

619

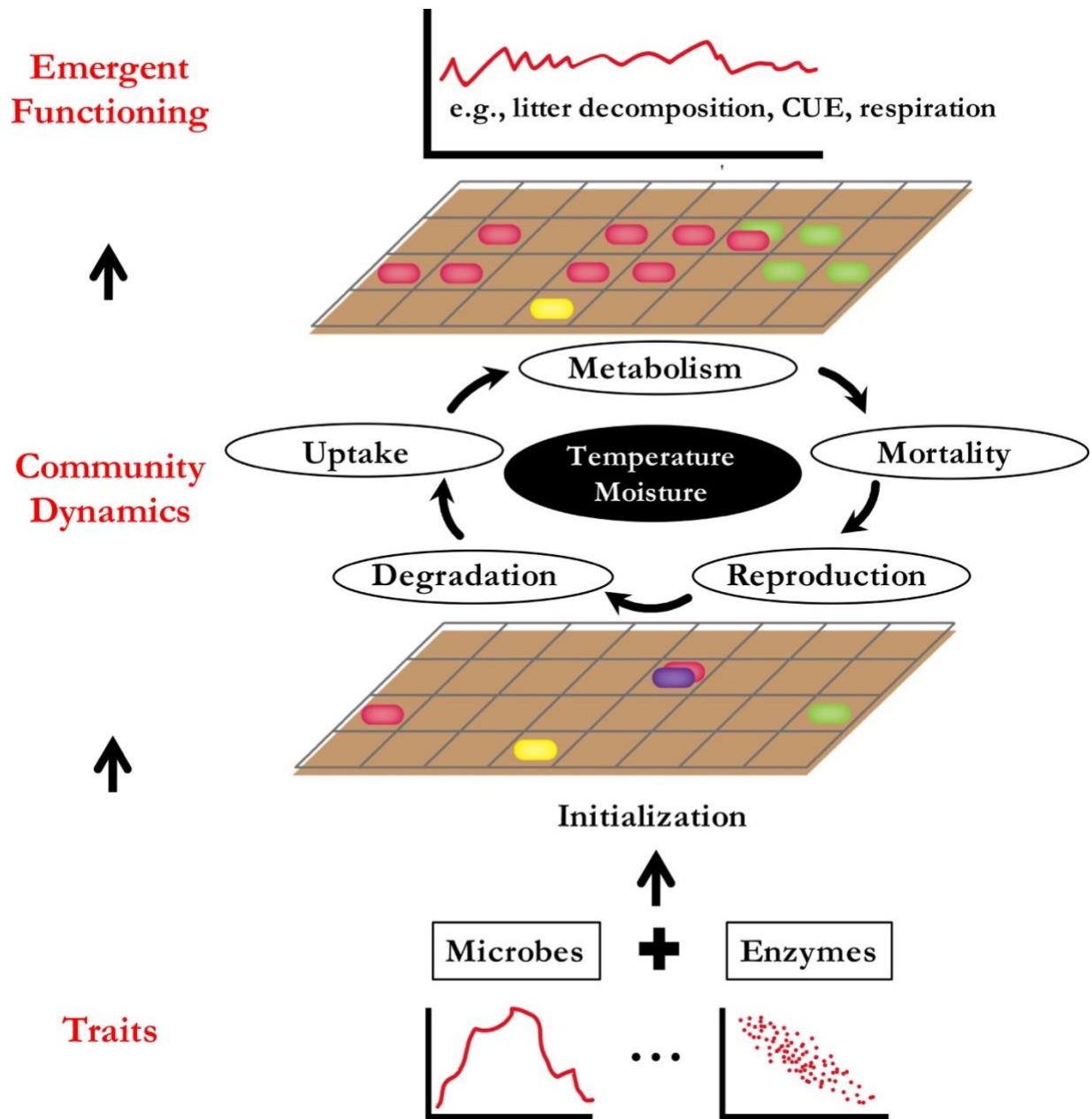
620

621

622

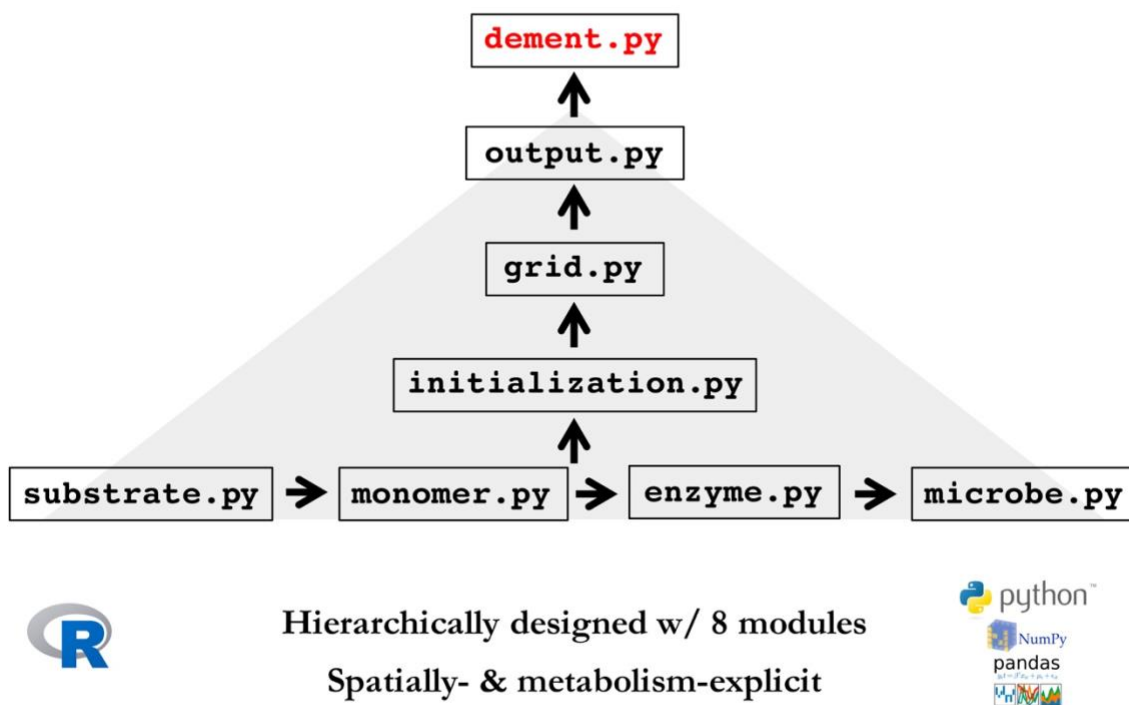
623

624



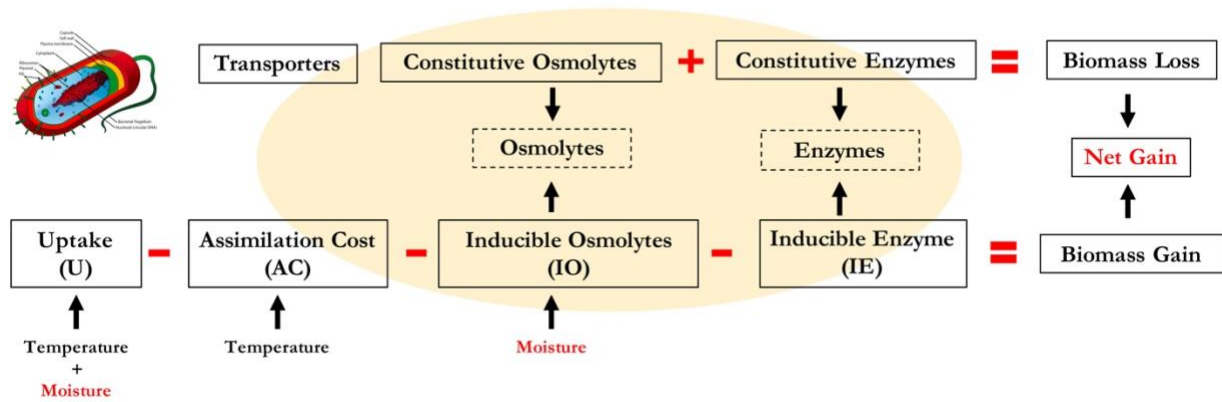
Supporting Fig. 1 DEMENTpy conceptual structure.

DEMENTpy Programming Structure

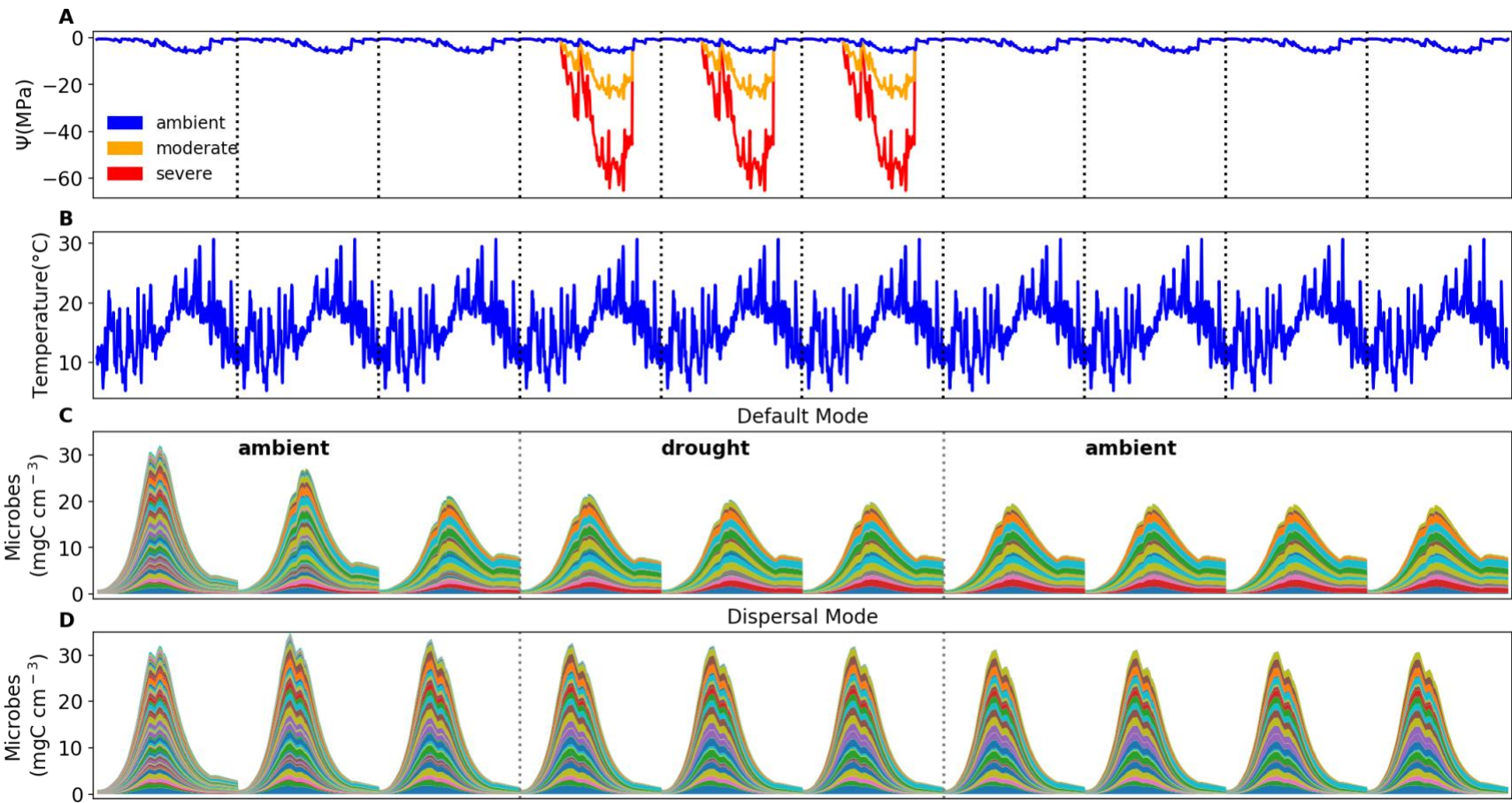


Supporting Fig.2 DEMENTpy programming structure. DEMENTpy emerges from restructuring and updating DEMENT programmed in R.

Framework of Metabolism Modelling



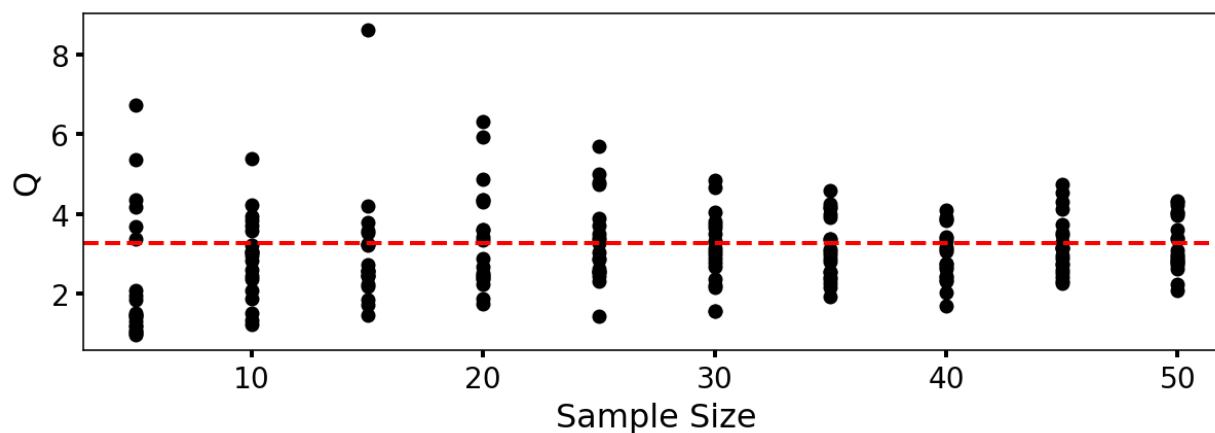
Supporting Fig.3 Schematic of intra-cellular processes simulated in DEMENTpy.



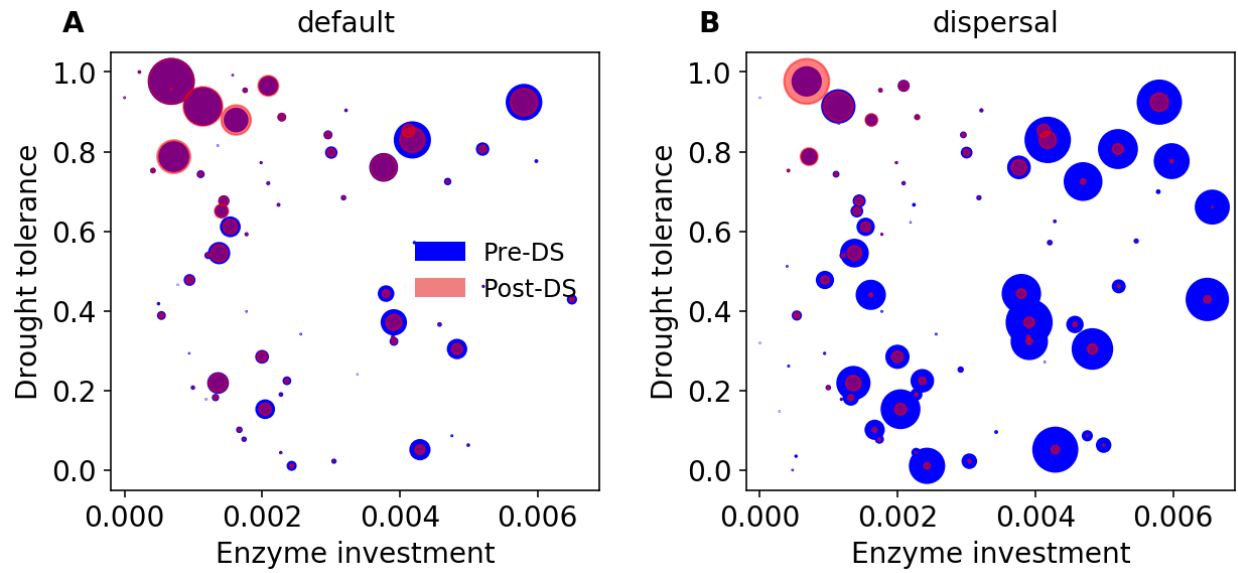
635

636 **Supporting Fig. 4 Environmental forcing and microbial community dynamics.** (A) Ambient daily water potential of 2011, with the
 637 orange and red line denoting the moderate and severe drought scenario, respectively, which were simply manipulated values by
 638 multiplying the water potential across the dry season from April through September by 4 and 10. (B) The corresponding daily
 639 temperature. (C, D) Microbial community dynamics of the default vs. dispersal model over 10 years under the ambient drought scenario.

640 The simulation experiences three phases as separated by the dashed grey lines: a spin-up phase of three years to realize relatively stable
641 community; a disturbance phase of three years imposing different drought scenarios; and a final recovery phase after drought disturbance.
642 Colored bands represent different hypothetical taxa.



Supporting Fig. 5 DEMENTpy (v1.0) stochasticity convergence analysis. Q (quotient) is calculated as (90% percentile -10% percentile)/median with the data of degradation of substrates following [Bugmann et al. \(1998\)](#). Each sample size has 20 replicates that were randomly drawn from a sample pool of 112 runs. This analysis illustrates that a sample size of 40, which starts displaying relatively stabilized and converged variation, may be an appropriate choice considering a tradeoff of reliability vs. consumption of computing resource.



Supporting Fig. 6 Taxonomic changes in traits across dry season. (A) Taxon-specific traits of drought tolerance and enzyme investment of a microbial community without dispersal before (blue) and after the dry season (red) under the ambient scenario. (B) The same for a microbial community with dispersal. Each point corresponds to a different taxon, and the size is proportional to its biomass.